Superconductor–insulator transition in two-dimensional indium–indium-oxide composite

Bar Hen[a], Xinyang Zhang[b,c], Victor Shelukhin[a], Aharon Kapitulnik[b,c,d,1], and Alexander Palevski[a]

[a]School of Physics and Astronomy, Raymond and Beverly Sackler Faculty of Exact Sciences, Tel Aviv University, Tel Aviv 6997801, Israel; [b]Geballe Laboratory for Advanced Materials, Stanford University, Stanford, CA 94305; [c]Department of Applied Physics, Stanford University, Stanford, CA 94305; and [d]Department of Physics, Stanford University, Stanford, CA 94305

Contributed by Aharon Kapitulnik, October 26, 2020 (sent for review July 29, 2020; reviewed by Charles M. Marcus and Ronny Thomale)

The magnetic-field–tuned superconductor-to-insulator transition was studied in a hybrid system of superconducting indium islands, deposited on an indium oxide (InOx) thin film, which exhibits global superconductivity at low magnetic fields. Vacuum annealing was used to tune the conductivity of the InOx film, thereby tuning the inergrain coupling and the nature of the transition. The hybrid system exhibits a "giant" magnetoresistance above the magnetic-field–tuned superconductor-to-insulator transition (H-SIT), with critical behavior similar to that of uniform InOx films but at much lower magnetic fields, that manifests the duality between Cooper pairs and vortices. A key feature of this hybrid system is the separation between the quantum criticality and the onset of nonequilibrium behavior.

superconductor–insulator transition | quantum phase transition | granular superconductivity

Two-dimensional (2D) superconductor-to-insulator transitions (SITs) tuned by varying disorder, carrier density, or magnetic field have received much attention because they allowed for detailed exploration of the nature of these classes of quantum phase transitions (QPTs) as well as their proximate ground states (1–9). In particular, the magnetic-field–tuned SIT (H-SIT) appears to be broadly relevant to other classes of QPTs such as the quantum Hall-to-insulator transition (QHIT) (10), while it also can shed light on the anomalous transport behavior observed in many unconventional superconductors such as the high-Tc cuprates (6). In the conventional, purely bosonic picture of H-SIT, superconducting pairing amplitude persists through the transition into the insulating state, which is characterized as a condensate of delocalized vortices and localized Cooper pairs, whereas the superconducting state is a condensate of Cooper pairs with localized vortices. Quantum fluctuations of the phase of the superconducting order parameter control this QPT (11). On theoretical grounds, this approach is equivalent to a disordered array of superconducting islands coupled by Josephson junctions, where the amplitude fluctuations are ignored (12, 13). Thus, applying the conventional picture to experimentally studied material systems is strongly influenced by the film's effective morphology. Furthermore, strong disorder, even if microscopically homogeneous, can lead to strong inhomogeneities in the local superconducting pairing amplitude (14–16), which is further enhanced in the presence of magnetic field (17).

While the conventional picture failed to work in many experiments investigating H-SIT, exhibiting an intervening anomalous metallic phase that emerges as a "failed superconductor" (for a recent review see ref. 18), other material systems, notably amorphous indium oxide (InOx) (1, 4–6, 19) and titanium nitride (9), can be prepared to exhibit "direct" H-SIT. However, lack of proper thermalization (20) was observed as temperature is further reduced toward the transition in InOx (21) and TiN (22) experiments, a phenomenon that should be expected in studies of zero-temperature ground-state phases and quantum critical phenomena. While these observations led to proposals for novel insulating states that avoid the H-SIT altogether (23–25), Breznay et al. (19) proposed that the nonequilibrium difficulty can be circumvented by limiting the H-SIT studies in InOx films to temperatures where equilibrium and linear response are satisfied and then extrapolating the data to $T = 0$. However, it would still be desired to extend H-SIT studies in InOx by mitigating the nonequilibrium tendency to lower temperatures.

The conventional picture can be realized experimentally by artificially fabricating an inhomogeneous material system. Indeed, the importance of granularity in SIT has been recently explored in mesoscopic-scale ordered arrays of aluminum islands coupled by gated InGaAs/InAs two-dimensional electron gas (2DEG) (26) and of Sn islands coupled by a gated graphene substrate (27, 28), both emphasizing the occurrence of a metallic anomalous state. Thus, motivated by these studies, and focusing on elucidating the conventional Bose-dominated picture of H-SIT in ostensibly uniform InOx, we may attempt to enhance the inhomogeneity that emerges in the superconducting state by using pure indium islands where pair amplitude is robust, while leaving the weaker intergrain couplings that mediate global superconductivity to be the same as in uniform InOx.

In this paper we focus on demonstrating the importance of inhomogeneities in the InOx system by superimposing a granular structure of pure indium islands on a uniform thin film of continuous amorphous insulating InOx. The underlying InOx film is chosen to have resistance that, while insulating, can still allow for weak proximity coupling between the almost touching indium islands. Thus, while local superconductivity originates from the indium grains, global superconductivity below the

Significance

The magnetic-field–tuned superconductor-to-insulator transition (H-SIT) in disordered two-dimensional thin-film materials is paradigmatic for quantum phase transition. While in the standard approach pairing persists into the insulating phase, and the transition is driven by quantum phase fluctuations, the role of its associated inhomogeneous nature, particularly in the widely studied InOx system, remains an open question. Here we use a granular structure of pure indium islands where pairing amplitude is well defined, superimposed on a uniform thin film of barely insulating InOx, which provide the intergrain coupling, to preferentially gain insight into the role of phase fluctuations in InOx H-SIT. The robust pairing in the indium islands helps mitigate nonequilibrium effects that often disrupt the approach to H-SIT in InOx experiments.

Author contributions: B.H., A.K., and A.P. designed research; B.H., X.Z., and V.S. performed research; B.H., X.Z., V.S., A.K., and A.P. analyzed data; and B.H., A.K., and A.P. wrote the paper.

Reviewers: C.M.M., University of Copenhagen; and R.T., University of Würzburg.

The authors declare no competing interest.

[1]To whom correspondence may be addressed. Email: aharonk@stanford.edu.

Published December 30, 2020.

PHYSICS

H-SIT and the strong insulating behavior above it are controlled by the InOx film. The resulting sample configuration, particularly in the superconducting state where intergrain couplings dominate the physics, ensures the 2D nature of our samples. In addition, the large In grains with their robust pair amplitude help mitigate nonequilibrium effects that, as we pointed out, often disrupt the approach to H-SIT in InOx experiments. Contrasting this system with previously studied H-SIT platforms, particularly InOx, we are able to point to the key effects of the imposed granularity, which include the following: Unlike in uniform InOx, we 1) observe the emergence of granularity with the evolution of superconductivity in the individual In grains and 2) observe the establishment of phase coherence in a different, much lower temperature regime. 3) Since it originates from the indium grains through intergrain coupling via InOx barriers, the overall scale of magnetic fields is much lower in the present system, separating the H-SIT from any ambiguity of proximity to H_{c2}. 4) A Mott variable-range hopping (29) on both sides of the H-SIT in uniform InOx (19) is dominated by an Efros–Shklovskii mechanism (30) in the present granular system. 5) Finally, the envelope of equilibrium behavior in these composite films is much expanded over uniform InOx films, which allows for a study of the evolution toward strong nonequilibrium effects at low temperatures as a function of magnetic field, observing, e.g., that the transition to strong nonequilibrium state is only weakly temperature dependent. These observations sharpen the applicability of the conventional boson-dominated approach for the understanding of direct H-SIT.

Results

The results presented below are focused on low-temperature resistivity, measured in killo-Ohm per square (k$\Omega/\square$) of Sample1-second anneal and Sample2-first anneal both being the closest to the SIT critical point from the superconducting side.

The cooling curve (Fig. 1, *Inset*) of sample 1–second anneal shows a negative temperature coefficient of the resistivity (TCR) ($d\rho/dT < 0$) corresponding to an insulating behavior in the temperature range of 70 to 3.4 K. Then, at the transition temperature of pure indium, $T_c^{\mathrm{In}} = 3.4$ K, the resistivity drops by $\sim 10\%$ followed by a slight increase which is attributed to the insulating behavior of the InOx. For temperatures below $\sim$2K the TCR changes sign again, resulting in a full superconductivity of the film with zero resistance below 0.5 K. This sample is the closest to the SIT from the superconducting side in our set.

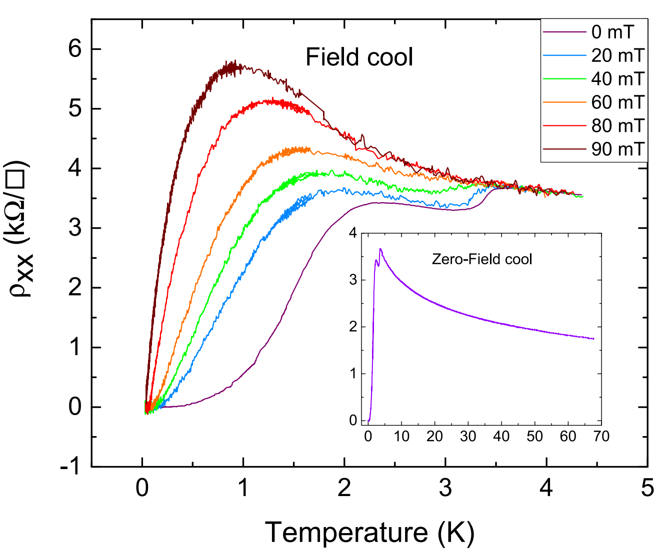

Fig. 1. Low-temperature cooling curves at low magnetic fields for sample 1–second anneal. A two-step transition is clearly observed at very low fields. *Inset* depicts the insulating behavior at zero magnetic field and higher temperatures followed by the superconductor transition. Note that above T_c of the In grains (3.4 K), the resistivity returns to the normal-state behavior, which continues below 3.4 K with high fields.

Low-temperature cooling curves of sample 1–second anneal at low magnetic fields are shown in Fig. 1 and further reveal the nature of the double-peak transition. While at $H = 0$ the first peak clearly coincides with T_c^{In}, this feature disappears and merges to the lower-temperature curve at $\gtrsim$70 mT. This is more than twice the critical field of pure type I superconducting In, demonstrating the decrease in mean free path in the thin-film form of the material (31), particularly reflecting the nanostructured nature of the individual grains, which were demonstrated to reach a critical field as large as 170 mT (32). Thus, the disappearance of the resistance drop with increasing magnetic field may not indicate the actual disappearance of superconductivity in the individual In islands. It most likely suggests that the positive TCR due to superconducting pairing susceptibility in the In grains is compensated by the negative TCR of the underlying InOx. Further increase of the magnetic field recovers the normal-state insulating behavior before a global decrease in the resistance as the combined system seems to tend toward a superconducting state at $T = 0$.

Upon further increase of magnetic field, the tendency to a superconducting state is suppressed, and an insulating behavior appears. As is clearly seen in Fig. 2, a transition from a superconducting to an insulating behavior is identified with the change in TCR from positive to negative, with a temperature-independent separatrix. The transition occurs at a critical resistance of $\sim$6.0 kΩ, which within the error bars of determining the sample's sheet resistance agrees with the quantum of resistance $\rho_Q = h/4e^2 \approx$ 6.5 kΩ.

Identifying the quantum SIT in the temperature-dependence data, we can further investigate the nature of the transition by studying the magnetoresistance isotherms. Performing the experiment at finite temperature, quantum dynamics that control the quantum phase transition are cut off by the finite temperature $k_B T$. The zero-temperature value of the critical conductivity, which in 2D does not contain a spatial scale, is multiplied by a scaling function of the ratio between the diverging length $\xi(H, D) \propto |H - H_c|^{-\nu}$ (here D represents a given realization of disorder) that controls the quantum phase transition and a thermal length that reflects the cutoff of the quantum dynamics by thermal fluctuations $\sim k_B T$. At H_c the argument of the scaling function must vanish for any finite temperature, giving rise to an isotherms-crossing point, a hallmark of H-SIT (11). However, an initial inspection of the magnetoresistance isotherms suggests that the higher-temperature data may be consistent with a higher critical field, where below $\lesssim$100 mK the true critical-field crossing point is identified. Indeed, as long as linear response prevails, the critical behavior needs to be determined in the limit of $T \to 0$. However, as noted in *Materials and Methods*, we observe a hierarchy of grain sizes, dominated by larger grains of average size $\sim$1,500 Å, which are responsible for the initial decrease in resistance at 3.4 K and thus dominate the higher-temperature resistive transition. Smaller grains that continue to exhibit amplitude fluctuations alter the true realization of the disorder, seemingly projecting a higher critical-field crossing point. As the temperature is lowered toward $T \to 0$, the full extent of the disorder embedded in the sample is realized, and the true quantum critical point at H_c takes over the critical behavior, as is clearly identified in the lowest-temperature data ($\lesssim$100 mK) shown in Fig. 3. That this is the "true" crossing point is also in agreement with a critical-field bound between 99.25 and 99.75 mT, which we determined from the temperature-dependence data (Fig. 2, *Inset*). Resistance vs. temperature measurements above H_c show

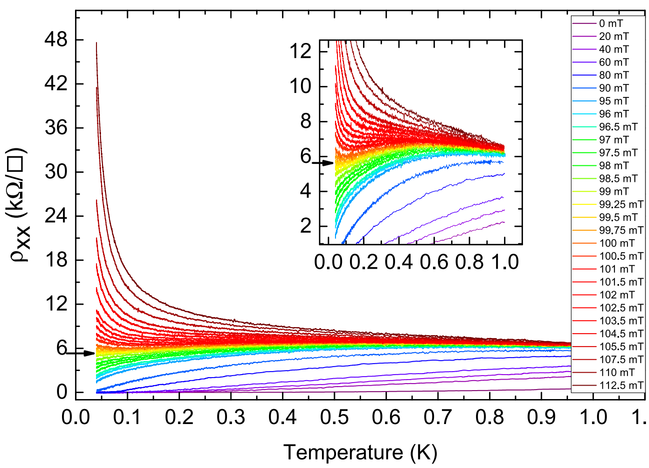

Fig. 2. Series of cooling curves of sample 1–second anneal at different magnetic fields indicating the SIT. The field which separates the superconducting and insulating curves, $H_c \approx 99.5$ mT, is marked by the arrow. For fields lower than H_c the sample becomes superconducting whereas for fields higher than H_c the sample becomes insulating.

insulating behavior, which further demonstrates that the secondary, higher-field critical point would not survive to $T = 0$. Establishing the H-SIT critical point, where both the temperature and field dependences agree, is further corroborated by calculating the length scale associated with this determination. Taking $\nu \approx 2.05$ (see below), even with the aforementioned uncertainty in critical field, we estimate a correlation length $\xi \approx \xi_0 |(99.75 - 99.25)/99.75|^{-2.05} \gg \xi_0$, which ensures that any "microscopic" length, e.g., if $\xi_0 \sim$ typical In grain size, is not affecting the sharpness of the transition. Finally, we note that the observed value of H_c, which is much smaller than previously observed in uniform InOx films, is a result of the source of pairing in our system, originating from the In grains. This in turn allows for a detailed study of the bosonic contribution to the magnetoresistance peak and the weak loss of pairing susceptibility with increasing field, as discussed below.

Turning to the higher-field regime of the magnetoresistance isotherms, the sample's resistance increases sharply to values that far exceed the fermionic metal-insulating threshold of $\sim$26 kΩ, indicating a strong bosonic behavior (11), similar to the behavior found in uniform InOx films (1, 4–6, 19). However, unlike uniform InOx films, here the underlying pairing originates from the In grains and is thus confined to much smaller range of magnetic fields. At the same time, vestiges of superconducting fluctuations are clearly observed at low temperatures even to the highest magnetic field measured. For example, at 1 T we find $\rho_{xx}(40\ \mathrm{mK})/\rho_{xx}(400\ \mathrm{mK}) \approx 2$, which is too large to be accounted for by the fermionic system only.

Data Analysis and Discussion

Studies of H-SIT in amorphous indium-oxide films have been a subject of intense research efforts for over 15 y, owing primarily to the giant positive magnetoresistance observed on the insulating side of the transition (4–6). Since superconductivity originates from a normal state with a (fermionic) sheet resistance of order a few k$\Omega/\Box$, the observation of a magnetoresistance peak in excess of $\sim$G$\Omega/\Box$ (33) must be interpreted as a consequence of localization of persisting Cooper pairs (11). Such a behavior is intrinsic to an array of Josephson-coupled grains, where intergrain coupling is controlled by gate tuning the conductance of substrate material, for example in 2DEG AlGaAs/GaAs (26) or graphene (27). Focusing on magnetic-field tuning SIT in InOx, the underlying InOx that serves as the coupling layer is estimated to have a normal-state sheet resistance of $\sim$10 k$\Omega/\Box$, which could only support weak local pairing, when proximitized from the indium grains. This in turn realizes strong separation between the strength of superconductivity in the In grains and that of the coupling in the InOx system.

The scaling analysis outlined above compares a diverging correlation length $\xi \propto |H - H_c|^{-\nu}$ on either side of the critical field, H_c, to a thermal length $L_T \sim (k_B T)^{-1/z}$ associated with the finite temperature that cuts off the quantum dynamics of the transition (z is the dynamical exponent). It is easy to arrive to a simple expression for the system's sheet resistance (11) near criticality:

$$\rho(H, T) = \rho_c \mathcal{F}\left(|H - H_c| T^{-1/z\nu}\right), \qquad \textbf{[1]}$$

where $\mathcal{F}(x)$ is a scaling function that depends on the distance to the critical field. Requiring that $\rho(H_c, 0) = \rho_c$, we must have $\mathcal{F}(0) = 1$, independent of temperature, which is a manifestation of the emerging crossing point in the measured field-dependent resistance isotherms.

For further analysis we focus on the data obtained for sample 1–second anneal which is the closest to the SIT from the superconductor side exhibiting zero resistance at zero magnetic field. To apply the above scaling in a consistent way we go back to Fig. 2, to determine that the isotherms near $H_c \approx 99.5$ mT seem to reach their low-temperature asymptotic value below $\sim$100 mK. Fig. 4*A* is a plot of the low-temperature data fitted to the form of Eq. **1**. The data collapse was achieved by adjusting the critical field and the complex exponent $z\nu$. Within the choice of temperature range and reduced magnetic field, we find that the data are best fitted with $H_c = 99.4 \pm 0.1$ mT and $z\nu = 2.05 \pm 0.10$. We note, however, that if we restrict ourselves to a much smaller reduced parameter, $x \lesssim 0.005$, the quality of the data is not good enough to rule out exponents as large as $z\nu \sim 2.5$.

Thus, to further investigate the critical behavior we use a different test of the scaling near the H-SIT, which was recently introduced by Breznay et al. (19). Starting on the insulating side of the transition, we consider it most likely that the resistance is dominated by variable-range hopping (VRH) of Cooper pairs. To have a simple expression which connects smoothly with the scaling analysis at the H-SIT (Eq. **1**), we take

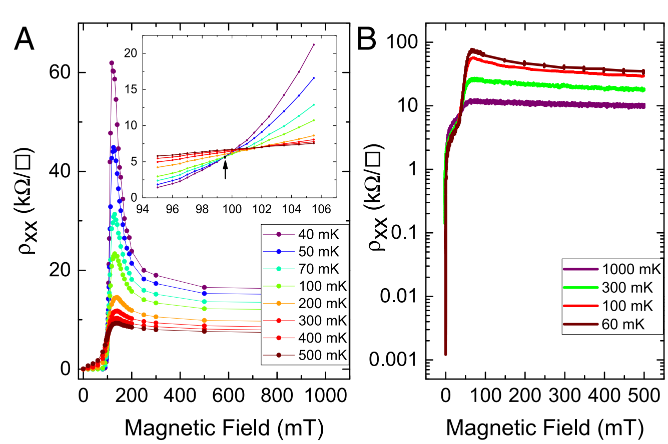

Fig. 3. (*A* and *B*) Magnetoresistance at different temperatures of (*A*) sample 1–second anneal and (*B*) sample 2–first anneal. Both of the samples exhibit H-SIT with a well-pronounced peak in the insulating phase. The magnetoresistance of sample 1–second anneal in *A* was deduced from Fig. 2. *A*, *Inset* zooms in the critical-field region where the curves intersect which is a hallmark of 2D quantum SIT. H_c for the low-temperature range of $\lesssim$100 mK is marked by a black dot and arrow.

PHYSICS

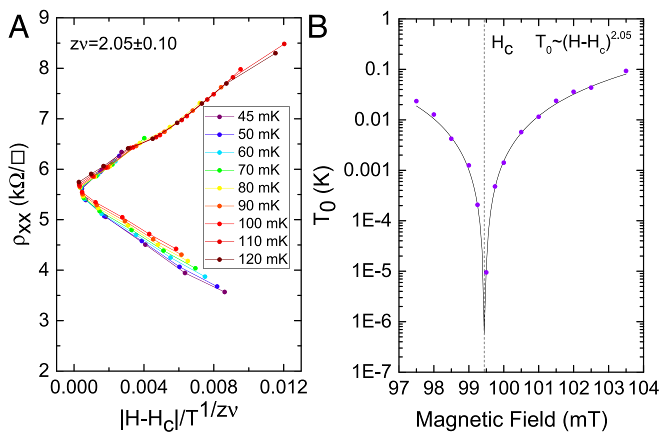

Fig. 4. Verification of the scaling laws of the SIT in sample 1–second anneal. (*A*) Scaling of isotherms near H_c for $z\nu = 2.05$. (*B*) The characteristic temperatures extracted from the fits to Eqs. **2** and **3** as a function of magnetic field, showing a critical behavior at H_c consistent with the determined critical exponent.

$$\rho_{xx}(T,H) \approx \rho_c \exp[(T_0(H)/T)^{\delta}] \text{ for } H > H_c \qquad [2]$$

with δ describing the nature of the VRH that governs the electronic transport.

On the superconducting side, for $H < H_c$, we expect that the longitudinal resistivity will be dominated by motion of vortices. Assuming Cooper pairs–vortex duality, the (measured) conductivity tensor $\underline{\sigma}$ is related to the vortex-resistivity tensor $\underline{\rho}^v$ according to $\underline{\sigma} = (4e^2/h)^2 \underline{\rho}^v$, implying that (34)

$$\rho_{xx} = (4e^2/h)^2 \sigma^v_{xx} = \rho_c \exp[-(T_0(H)/T)^{\delta}], \qquad [3]$$

where we expect vortex VRH below H_c to replace Cooper-pairs VRH above H_c (19). Consistency between Eqs. **1** and **3** requires that $T_0(H) \propto |H - H_c|^{z\nu}$. Fig. 4*B* is a result of fitting Eqs. **1** and **2** to the data and extracting the characteristic temperature-scale $T_0(H)$. The fit yields the same $H_c = 99.4$ mT and a scaling exponent $z\nu = 2.05 \pm 0.10$ as in Fig. 4*A*. We emphasize that very close to the critical point Eqs. **2** and **3** should be considered as interpolation equations that need to exhibit consistency, while not necessarily a demonstratable exponential behavior (19).

The study of ρ_{xx} on the insulating side also allows for the detection of the transition to the nonequilibrium state where electrons fail to fully thermalize with the lattice. To observe that transition we continue to assume the form of Eq. **2** and thus plot $\ln[\ln(\rho_{xx}/\rho_c)]$ vs. $\ln(1/T)$. Such a plot allows us to confirm the exponent $\delta \approx 1/2$ discussed above (30) (which was determined in a direct fit to Eq. **2**), and it also allows us to observe the increase of that exponent at low temperatures, away from the H-SIT.

Fig. 5 depicts this evolution for magnetic fields above H_c. As the temperature is reduced, a gradual crossover with an intermediate "simple activation" behavior with $\delta = 1$ is observed, followed by a "superactivation" behavior, where a strong decoupling of the electronic system from the lattice occurs with $\delta > 1$. We emphasize that the data points which were used for Fig. 4*B* were taken only from the temperature range where $\delta = 1/2$ can fit reasonably well. While the deviation from VRH depends on the proximity to the H-SIT. It is important to note that the initial deviation from VRH depends on temperature—the closer the field is to H_c (and hence the resistance to ρ_c), the lower the temperature of that crossover. However, the full transition to superactivation is no longer dependent on the proximity to the H-SIT, but is rather an intrinsic property of the sample and only weakly temperature dependent, where for the sample shown in Fig. 5 it occurs at $T_{Neq} \sim 30$ mK.

Indeed, such superactivation behavior, which is often accompanied by strong nonlinear and hysteretic $I - V$, was studied in detail, particularly in InOx (25), where the analyses were often guided by different theoretical approaches (23, 24). However, in the present study we are able to limit our discussion to linear response and thus to temperatures and magnetic field close to the SIT, where fits to the scaling functions Eqs. **2** and **3**, with $\delta \approx 0.5$, work well. For temperatures below where $\delta = 0.5$ works, we see a continuous progression of the slope with decreasing temperature. The transition from $\delta \le 1$ to $\delta > 1$ is understood as one possible way to quantify the location of this change in behavior.

Summary and Conclusions

In this paper we introduced a material system for the study of magnetic-field–tuned superconductor to insulator transition. Utilizing an underlying amorphous indium-oxide layer to control the coupling between a subsequently deposited film of pure indium islands, we create a unique granular system where the coupling between the grains can be controlled by careful annealing of the composite system in vacuum. Tuning the coupling to lie just at the borderline where superconductivity in the underlying InOx is suppressed, which is also close to the metal–insulator transition of InOx, the hybrid system allows for a careful study of an H-SIT in a system with well-established superconducting pairing amplitude (pure In) and InOx mediating the intergrain coupling. This system exhibits all of the features of a direct H-SIT, including a "giant" magnetoresistance above the H-SIT, with critical behavior that manifests the duality between Cooper pairs and vortices. The transport behavior in the superconducting and insulating phases proximate to the H-SIT is shown to be dominated by interaction-mediated variable-range hopping, as is expected for a granular system. Finally, as the envelope of equilibrium behavior in this composite film is much expanded over uniform InOx films, it allows for a study of the evolution toward strong nonequilibrium effects at low temperatures as a function of magnetic field, suggesting that a transition to a strong nonequilibrium state is only weakly temperature dependent.

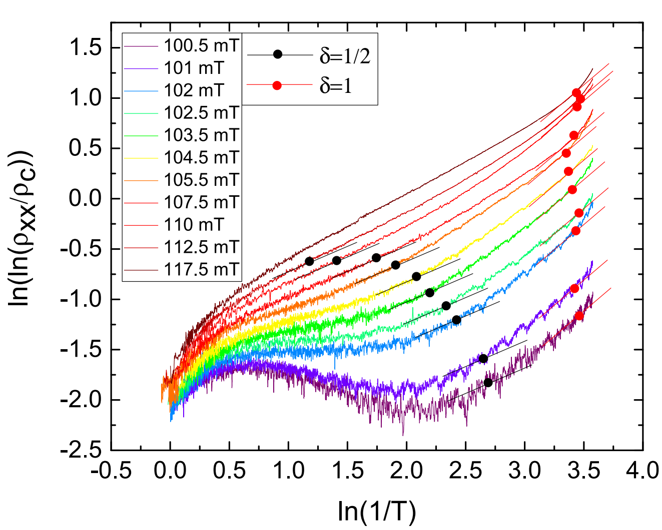

Fig. 5. A rough determination of the crossover temperature from equilibrium VRH behavior to the nonequilibrium state of sample 1–second anneal. Black circles denote the first deviation from VRH with $\delta = 1/2$, whereas red circles denote the crossover to "superactivation" with $\delta > 1$.

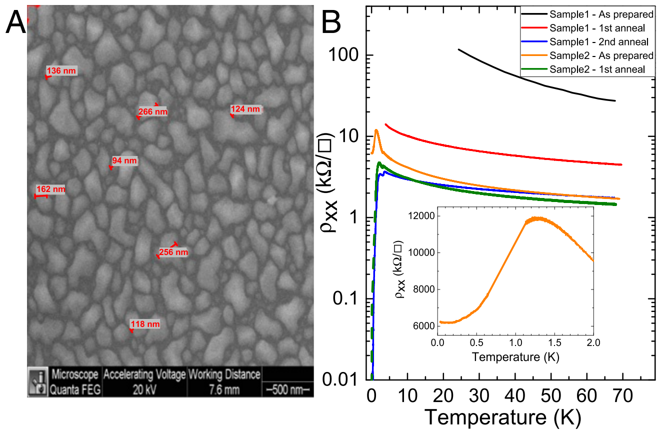

Fig. 6. Sample characterization. (*A*) SEM image of sample 1 confirming the granular (discontinuous) structure of the In on top of the amorphous InOx. The average size of the grains is 1,500 Å. (*B*) Film resistance versus temperature for both samples. The desired range of the resistance is obtained by tuning the intergrain coupling using annealing. *Inset* shows the low-temperature dependence of sample 2–as prepared. While this sample shows a drop in resistance toward a superconducting state, it fails to complete this transition, ending up saturating at a value close to $h/4e^2$ (this regime of coupling is not discussed in the present paper). The first anneal seems to exhibit a superconducting transition very close to $T = 0$.

Materials and Methods

Our system consists of in situ evaporated In islands on top of a thin film of InOx. For our study we employed two different substrates. Semiinsulating GaAs was used for sample 1 whereas lithium-ion glass ceramics (Li-ICGC) (MTI Corp.) substrate allowing electrostatic gating was used for sample 2. A 300-Å continuous layer of amorphous InOx was deposited onto these substrates using an In_2O_3 pallet, in an oxygen atmosphere at pressure of 5×10^{-5} Torr and at a slow rate of $\sim$0.5 to 1 Å/s. Then, the layer was covered by In islands by evaporating pure indium, at base pressure of 5×10^{-7} Torr and at a rate of $\sim$20 Å/s. The crystalline structure of the granular In film was confirmed by scanning electron microscopy (SEM) imaging (Fig. 6*A*), whereas within the SEM resolution we could not observe any grains of InOx. While we observe a hierarchy of grain sizes, the coverage of the film is dominated by grains of average size $\sim$1,500 Å as determined by scanning along horizontal cuts of Fig. 6*A*. This is expected to dominate the onset of local superconductivity as is discussed below. At the same time, the islands do not coalesce, thus forcing the InOx barriers to determine global superconductivity through intergrain Josephson coupling. This feature ensures the two-dimensionality nature of global superconductivity in the films, which will be our starting point in the analyses of the data.

Contacts were made using e-beam evaporation of Au-Ti on the corners of the samples, enabling transport measurements in Van der Pauw configuration. Aiming to obtain InOx films on the insulating side of the metal–insulator transition (MIT), as prepared films showed immeasurably high values of resistivity at low temperatures. Heating in vacuum for a few hours at $\sim$55 °C changed the oxygen concentration in the InOx (5, 6) without affecting the In islands, thus allowing for control over the conductance of the intergrain coupling, which in turn determined the overall transport response and in particular the nature of the H-SIT. The annealing process was used for several InOx platforms; however, some of the more dramatic SIT effects were obtained for a combined room-temperature sheet resistance of $\rho_N \sim 0.9$ k$\Omega/\square$, which is the type of samples we discuss in this paper (Fig. 6*B*). Subsequent transport measurements were performed in a dilution refrigerator in a wide temperature range (28 mK to 70 K) and in magnetic fields up to 1 T, which was sufficient to suppress the superconducting state in the samples.

Data Availability. The data have been deposited in GitHub, https://github.com/barhen0510/Superconductor-insulator-transition-in-two-dimensional-indium-indium-oxide-composite.

ACKNOWLEDGMENTS. We acknowledge important discussions with Boris Spivak and Steven Kivelson. Work at Stanford University was supported by the NSF Grant NSF-DMR-1808385. Work at Tel Aviv University was supported by the Israeli Science Foundation (Grant 277/16), the Israel Ministry of Science and Technology (Contract 67091), the US–Israel Binational Science Foundation (Grant 2014098), and the Wolfson Applied Materials Research Center (Tel Aviv University).

1. A. F. Hebard, M. A. Paalanen, Magnetic-field-tuned superconductor-insulator transition in two-dimensional films. *Phys. Rev. Lett.* **65**, 927–930 (1990).
2. A. Yazdani, A. Kapitulnik, Superconducting-insulating transition in two-dimensional *a*-moge thin films. *Phys. Rev. Lett.* **74**, 3037–3040 (1995).
3. D. Ephron, A. Yazdani, A. Kapitulnik, M. R. Beasley, Observation of quantum dissipation in the vortex state of a highly disordered superconducting thin film. *Phys. Rev. Lett.* **76**, 1529–1532 (1996).
4. V. F. Gantmakher, M. V. Golubkov, V. T. Dolgopolov, G. E. Tsydynzhapov, A. A. Shashkin, Destruction of localized electron pairs above the magnetic-field-driven superconductor-insulator transition in amorphous In-O films. *JETP Lett.* **68**, 363–369 (1998).
5. G. Sambandamurthy, L. W. Engel, A. Johansson, D. Shahar, Superconductivity-related insulating behavior. *Phys. Rev. Lett.* **92**, 107005 (2004).
6. M. Steiner, A. Kapitulnik, Superconductivity in the insulating phase above the field-tuned superconductor-insulator transition in disordered indium oxide films. *Phys. C Supercond.* **422**, 16–26 (2005).
7. N. Marković, C. Christiansen, A. M. Goldman, Thickness–magnetic field phase diagram at the superconductor-insulator transition in 2D. *Phys. Rev. Lett.* **81**, 5217–5220 (1998).
8. E. Bielejec, W. Wu, Field-tuned superconductor-insulator transition with and without current bias. *Phys. Rev. Lett.* **88**, 206802 (2002).
9. T. I. Baturina *et al.*, Superconductivity on the localization threshold and magnetic-field-tuned superconductor-insulator transition in TiN films. *JETP Lett.* **79**, 337–341 (2004).
10. S. L. Sondhi, S. M. Girvin, J. P. Carini, D. Shahar, Continuous quantum phase transitions. *Rev. Mod. Phys.* **69**, 315–333 (1997).
11. M. P. A. Fisher, Quantum phase transitions in disordered two-dimensional superconductors. *Phys. Rev. Lett.* **65**, 923–926 (1990).
12. M. Wallin, E. S. Sorensen, S. M. Girvin, A. P. Young, Superconductor-insulator transition in two-dimensional dirty boson systems. *Phys. Rev. B* **49**, 12115–12139 (1994).
13. H. Khan, N. Trivedi, Local spectroscopies across the superconductor-insulator transition. *Phys. Rev. B* **99**, 144516 (2019).
14. A. Ghosal, M. Randeria, N. Trivedi, Role of spatial amplitude fluctuations in highly disordered *s*-wave superconductors. *Phys. Rev. Lett.* **81**, 3940–3943 (1998).
15. A. Ghosal, M. Randeria, N. Trivedi, Inhomogeneous pairing in highly disordered s-wave superconductors. *Phys. Rev. B* **65**, 014501 (2001).
16. Y. Dubi, Y. Meir, Y. Avishai, Nature of the superconductor-insulator transition in disordered superconductors. *Nature* **449**, 876–880 (2007).
17. E. Shimshoni, A. Auerbach, A. Kapitulnik, Transport through quantum melts. *Phys. Rev. Lett.* **80**, 3352–3355 (1998).
18. A. Kapitulnik, S. A. Kivelson, B. Spivak, Colloquium: Anomalous metals: Failed superconductors. *Rev. Mod. Phys.* **91**, 011002 (2019).
19. N. P. Breznay, M. A. Steiner, S. A. Kivelson, A. Kapitulnik, Self-duality and a Hall-insulator phase near the superconductor-to-insulator transition in indium-oxide films. *Proc. Natl. Acad. Sci. U.S.A.* **113**, 280–285 (2016).
20. B. L. Altshuler, V. E. Kravtsov, I. V. Lerner, I. L. Aleiner, Jumps in current-voltage characteristics in disordered films. *Phys. Rev. Lett.* **102**, 176803 (2009).
21. M. Ovadia, B. Sacépé, D. Shahar, Electron-phonon decoupling in disordered insulators. *Phys. Rev. Lett.* **102**, 176802 (2009).
22. T. I. Baturina, A. Y. Mironov, V. M. Vinokur, M. R. Baklanov, C. Strunk, Localized superconductivity in the quantum-critical region of the disorder-driven superconductor-insulator transition in TiN thin films. *Phys. Rev. Lett.* **99**, 257003 (2007).
23. D. M. Basko, I. L. Aleiner, B. L. Altshuler, Possible experimental manifestations of the many-body localization. *Phys. Rev. B* **76**, 052203 (2007).
24. V. M. Vinokur *et al.*, Superinsulator and quantum synchronization. *Nature* **452**, 613–615 (2008).
25. M. Ovadia *et al.*, Evidence for a finite-temperature insulator. *Sci. Rep.* **5**, 13503 (2015).
26. C. G. L. Bottcher *et al.*, Superconducting, insulating and anomalous metallic regimes in a gated two-dimensional semiconductor-superconductor array. *Nat. Phys.* **14**, 1138–1144 (2018).
27. A. Allain, Z. Han, V. Bouchiat, Electrical control of the superconducting-to-insulating transition in graphene-metal hybrids. *Nat. Mater.* **11**, 590–594 (2012).
28. Z. Han *et al.*, Collapse of superconductivity in a hybrid TiN-graphene Josephson junction array. *Nat. Phys.* **10**, 380–386 (2014).
29. N. F. Mott, Conduction in glasses containing transition metal ions. *J. Non-Cryst. Solids* **1**, 1–17 (1968).
30. A. L. Efros, B. I. Shklovskii, Coulomb gap and low-temperature conductivity of disordered systems. *J. Phys. C Solid State Phys.* **8**, L49–L51 (1975).
31. R. D. Chaudhari, Critical magnetic fields in superconducting films of indium. *Phys. Rev.* **151**, 96–100 (1966).
32. N. Y. Mikhailin, S. G. Romanov, Y. A. Kumzerov, A. V. Fokin, D. V. Shamshur, Superconducting properties of indium nanostructured in pores of thin films of SiO2 microspheres. *Phys. Solid State* **60**, 1942–1947 (2018).
33. B. Sacépé *et al.*, High-field termination of a Cooper-pair insulator. *Phys. Rev. B* **91**, 220508 (2015).
34. A. Auerbach, D. P. Arovas, S. Ghosh, Quantum tunneling of vortices in two-dimensional condensates. *Phys. Rev. B* **74**, 064511 (2006).